X-Ray Binaries

End Stages of Stellar Evolution, IV

Stars end their life as one of three kinds of different compact objects:

White Dwarf: $\rho \sim 10^5 \ldots 10^6\,\mathrm{g\,cm^{-3}}$, $R \sim R_\oplus$, Equilibrium between gravitation and pressure from degenerate electrons, $M < 1.44\,M_\odot$ (Chandrasekhar-limit; 1931).

Neutron Star: $\rho \sim 10^{13} \ldots 10^{16}\,\mathrm{g\,cm^{-3}}$, $R \sim 10\,\mathrm{km}$, this density causes inv. β-decay ($\mathrm{p} + \mathrm{e}^- \rightarrow \mathrm{n}$), i.e., star consists (mainly) of neutrons. $1.44\,M_\odot < M \lesssim 3\,M_\odot$ (Oppenheimer-Volkoff limit; 1939).

Black Hole: For $M \gtrsim 3\,M_\odot$ no stable configuration known
$\Longrightarrow$ Star collapses completely
$\Longrightarrow$ Black Hole
Size scale: $R_\mathrm{S} = 2GM/c^2 = 3(M/M_\odot)\,\mathrm{km}$

Detectability, I

Sirius A+B (McDonald Observatory)

Luminosity of a sphere of radius R and temperature T:

$$L = 4\pi R^2 \cdot \sigma_\mathrm{SB} T^4 \qquad (6.1)$$

($\sigma_\mathrm{SB} = 5.67 \times 10^{-5}\,\mathrm{erg\,cm^{-2}\,K^{-4}\,s^{-1}}$)

For a typical white dwarf,
$R \sim 6000\,\mathrm{km}$, $T \sim 10000\,\mathrm{K}$
$\Longrightarrow L = 2.6 \times 10^{30}\,\mathrm{erg\,s^{-1}} \sim 6.6 \times 10^{-4}\,L_\odot$ corresponding to an absolute magnitude of $M_\mathrm{WD} = 15.9\,\mathrm{mag}$.
$\Longrightarrow$ with a limiting magnitude of 25 mag for today's telescopes, isolated WDs are detectable out to $\sim$700 pc.

First discovery: Alvan Graham Clark, 1862

Detectability, II

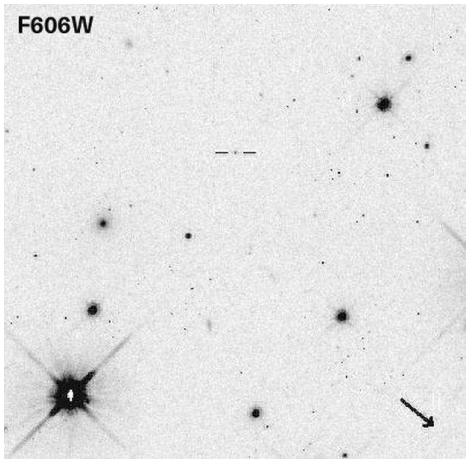

($17.5' \times 17.5'$ Walter & Matthews, 1997, Fig. 1)

Same calculation for a neutron star ($R = 10\,\mathrm{km}$, $T = 10^6\,\mathrm{K}$) gives $L_\mathrm{NS} \sim 7 \times 10^{28}\,\mathrm{erg\,s} \sim 2 \times 10^{-5}\,L_\odot$, or an absolute magnitude of 19.7 mag.
Pre VLT/Keck: practical limit of surveys $\sim$20 pc, 10 m class and space based telescopes of today extend this to $\sim$100 pc.

$\Longrightarrow$ It is virtually impossible to discover isolated neutron stars in the optical.

HST Image of the isolated neutron star RX J185635−3754, which has a visual magnitude $\sim$25.6 mag

Discovery of X-ray Binaries, I

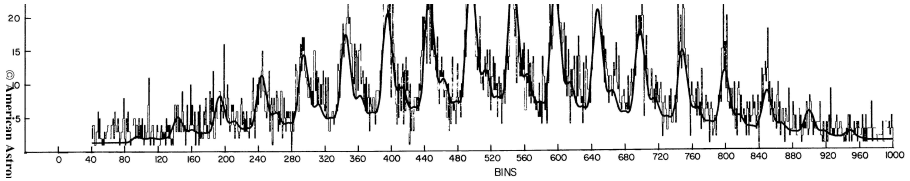

(Schreier et al., 1972, Fig. 4a)

Schreier et al. (1972): Detection of 4.8 s pulsations from Centaurus X-3 with *UHURU*: Cen X-3 is an X-ray Pulsar.

$\Longrightarrow$ at least some X-ray sources are rotating.

Discovery of X-ray Binaries, II

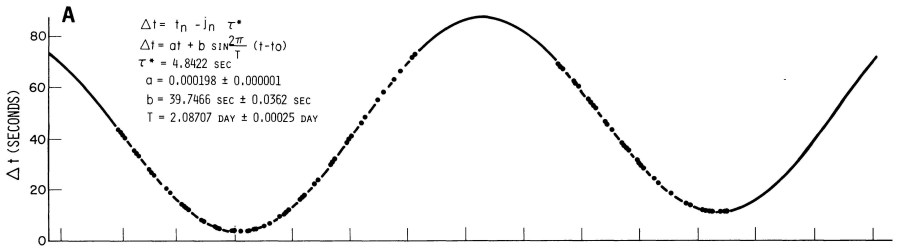

(Schreier et al., 1972, Fig. 4a)

Schreier et al. (1972): Time delay in arrival time of pulses from Cen X-3:

Cen X-3 is an X-ray Pulsar.

Discovery of X-ray Binaries, III

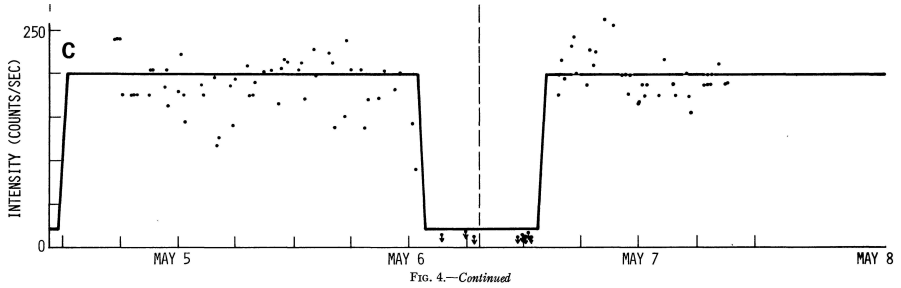

FIG. 4.—*Continued*

(Schreier et al., 1972, Fig. 4c)

Schreier et al. (1972): Cen X-3 shows periodic drops in X-ray count rate on a timescale of 2.08 d.

$\Longrightarrow$ eclipses by a star?

SOURCE IN HERCULES (2U1705+34)
November 6, 1971

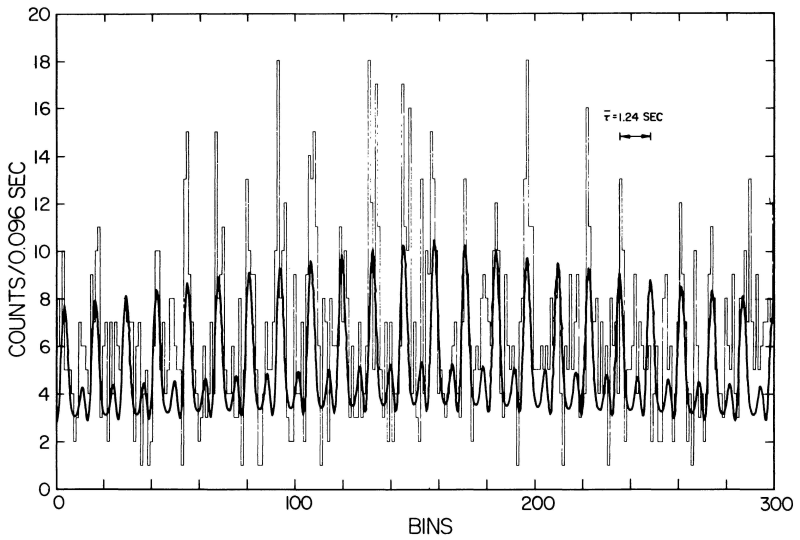

(Tananbaum et al., 1972, Fig. 1)

Detection of 1.24 s pulsations from Hercules X-1 with *UHURU*:

$\Longrightarrow$ X-ray pulsars as class of objects

Discovery of X-ray Binaries, V

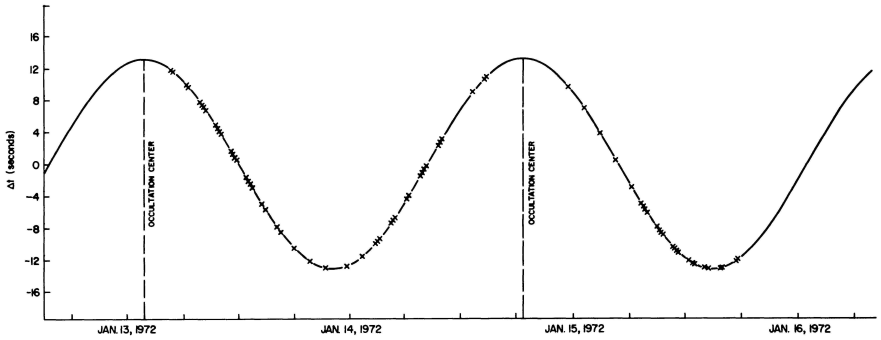

(Tananbaum et al., 1972, Fig. 3)

Similar to Cen X-3, X-ray pulsations of Her X-1 show periodic delays

(timescale: 1.7 d)

$\Longrightarrow$ X-ray binaries as class of objects

Discovery of X-ray Binaries, VI

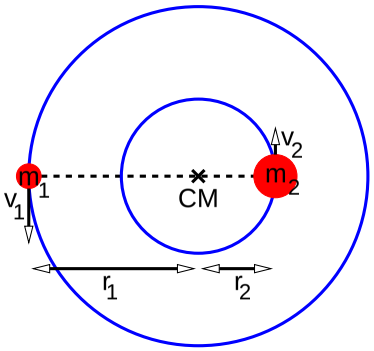

The delays seen in Cen X-3 and Her X-1 are ∼sinusoidal $\Longrightarrow$ assume circular orbit for simplicity
Observed velocity component $\perp$ sky:

$$v_{1,\mathrm{obs}} = v_1 \sin i = \frac{2\pi r_1}{P}\sin i = \frac{2\pi r}{P}\frac{m_2}{m_1+m_2}\sin i \quad (6.2)$$

where i is the system's inclination ($i = 90°$ is an "edge on orbit"). Combining Eq. (6.2) with Kepler's 3rd law,

$$\frac{r^3}{P^2} = \frac{G}{4\pi^2}(m_1+m_2) \quad (6.3)$$

gives the mass function

$$\frac{m_2^3 \sin^3 i}{(m_1+m_2)^2} = \frac{P v_1^3}{2\pi G} := f_M \quad (6.4)$$

The mass function gives a *lower limit* for m_2 using only the period P and the velocity amplitude, v_1, of the other object.

Hercules X-1: observed time delay: $\Delta t = 13.19\,s \Longrightarrow$ orbital radius $r_1 = c\Delta t = 4 \times 10^6$ km and a velocity of $v_1 \sim 170\,\mathrm{km\,s^{-1}}$. Since eclipses have been observed $i \sim 90°$. Therefore, the mass function of Her X-1 is $f_M = 1.75 \times 10^{33}\,\mathrm{g} = 0.876\,M_\odot$ (better measurements give $M = 1.44\,M_\odot$).

Black Hole Binaries, I

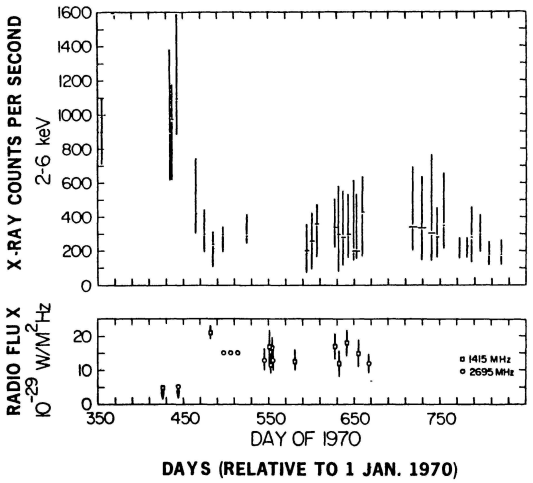

In Cyg X-1, no coherent periodicities were found.

However, Cyg X-1 showed correlated behavior in the radio and in the X-rays

$\Longrightarrow$ source localization, counterpart is HDE 226868, an O-star

(Murdin & Webster, 1971; Hjellming & Wade, 1971)

Black Hole Binaries, II

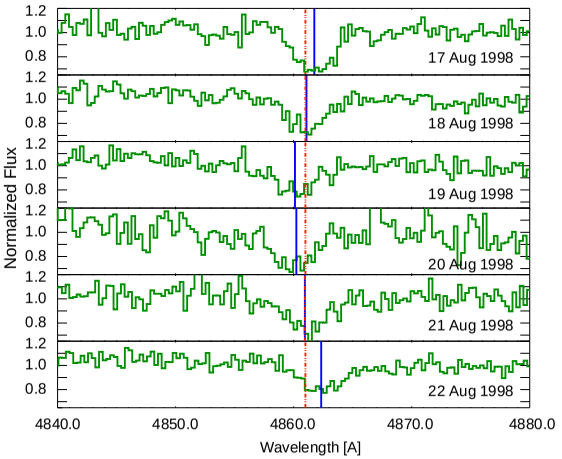

Motion of the Hβ line in HDE 226868/Cyg X-1
(Pottschmidt, Wilms)

For Cygnus X-1, the mass function is $f_M = 0.252\,M_\odot$, however, the companion is an O-star with $> 10\,M_\odot$, and this puts a lower limit of $\sim 8\,M_\odot$ to the mass of the compact object (Webster & Murdin, 1972)

The X-ray emitting object in Cygnus X-1 is a black hole.

X-Ray Binaries

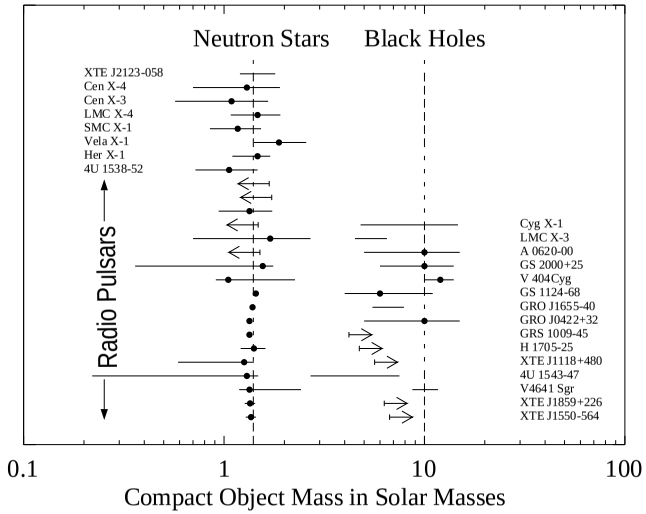

X-ray binaries are neutron stars or black holes accreting material from a normal star.

(Kalemci, priv. comm.)

Accretion, III

Why are X-ray binaries so bright?

1. Fusion

Reactions à la

$$4\mathrm{p} \longrightarrow {}^4\mathrm{He} + \Delta mc^2$$

Energy released:

Fusion yields
$\sim 6 \times 10^{18}\,\mathrm{erg\,g^{-1}} = 6 \times 10^{11}\,\mathrm{J\,g^{-1}}$

($\Delta E_{\mathrm{nuc}} \sim 0.007 m_{\mathrm{p}} c^2$)

2. Gravitation

Accretion of mass m from ∞ onto Black Hole M with radius R_{S} yields

$$\Delta E_{\mathrm{acc}} = \frac{GMm}{R_{\mathrm{S}}} \text{ where } R_{\mathrm{S}} = \frac{2GM}{c^2}$$

Accretion produces
$\sim 10^{20}\,\mathrm{erg\,g^{-1}} = 10^{13}\,\mathrm{J\,g^{-1}}$

($\Delta E_{\mathrm{acc}} \sim 0.1\, m_{\mathrm{p}} c^2$)

$\Longrightarrow$ Accretion of material is the most efficient astrophysical energy source.

. . . therefore accreting objects are the most luminous objects in the whole universe.

Roche Geometry, I

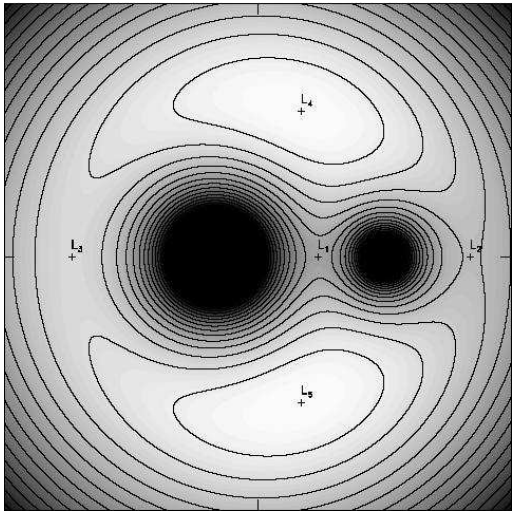

R. Hynes

Motion of gas in corotating frame around masses M_1, M_2 given by

$$\frac{d^2\boldsymbol{r}}{dt^2} + 2\boldsymbol{\omega} \times \frac{d\boldsymbol{r}}{dt} = -\frac{1}{\rho}\boldsymbol{\nabla} P - \boldsymbol{\nabla}\Phi$$

where the Roche potential:

$$\Phi_{\mathrm{R}}(\boldsymbol{r}) = -\frac{GM_1}{|\boldsymbol{r}-\boldsymbol{r}_1|} - \frac{GM_2}{|\boldsymbol{r}-\boldsymbol{r}_2|} - \frac{1}{2}(\boldsymbol{\omega}\times\boldsymbol{r})^2$$

and where

$$\boldsymbol{\omega} = \left(\frac{GM}{a^3}\right)^{1/2} \hat{e}$$

For X-ray binaries: one of the masses is a normal star the other is a compact object.

Roche Geometry, III

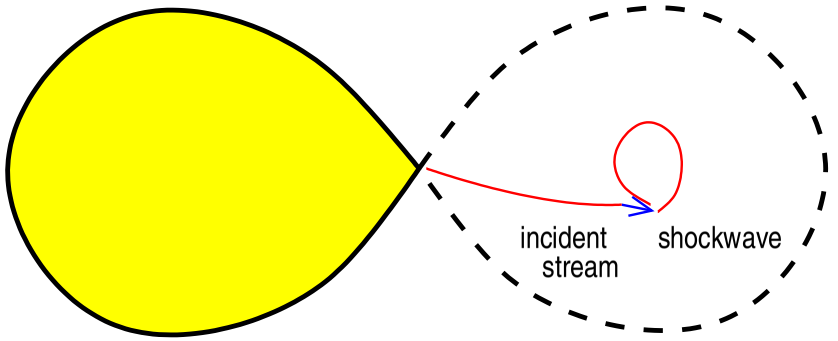

(after Lubow & Shu, 1975, Fig. 4)

Roche Lobe Accretion: Gas is transferred at inner Lagrange point.
Ballistic free fall towards compact object, forms elliptical orbit

Note: ellipse rotates because of Coriolis force!

Stream intersects $\Longrightarrow$ shock $\Longrightarrow$ randomization $\Longrightarrow$ circular orbit forms.

Material flows from normal star via inner Lagrange point, L_1, onto compact object

$\Longrightarrow$ formation of an accretion disk, with temperature $\sim 10^7$ K

$\Longrightarrow$ X-rays and Gamma-Rays.

Eddington luminosity, IV

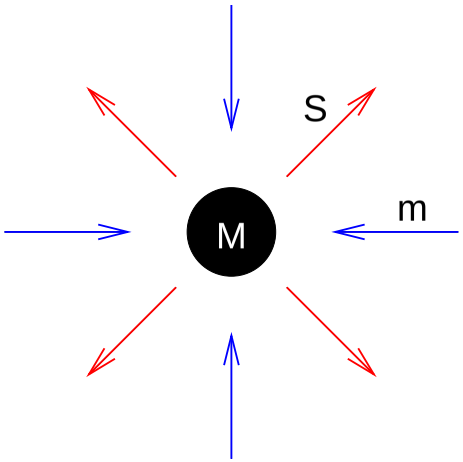

What is the maximum luminosity of an accreting object of mass M which is spherically symmetrically accreting ionized hydrogen gas?

At radius r, accretion produces energy flux S.

Important: Interaction between accreted material and radiation!

Eddington luminosity, VIII

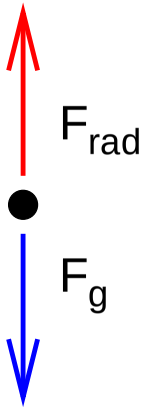

Force balance on accreted electrons and protons:

Inward force: gravitation:

$$F_\mathrm{g} = \frac{GMm_\mathrm{p}}{r^2} \tag{6.9}$$

Outward force: radiation force:

$$F_\mathrm{rad} = \frac{\sigma_\mathrm{T} S}{c} \tag{6.10}$$

where energy flux S is given by

$$S = \frac{L}{4\pi r^2} \tag{6.11}$$

where L: luminosity.

Note: $\sigma_\mathrm{T} \propto (m_\mathrm{e}/m_\mathrm{p})^2$, so negligable for protons.

But: strong Coulomb coupling between electrons and protons

$\Longrightarrow$ F_rad also has effect on protons!

Eddington luminosity, IX

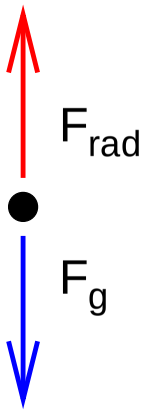

Accretion is only possible if gravitation dominates:

$$\frac{GMm_\mathrm{p}}{r^2} > \frac{\sigma_\mathrm{T} S}{c} = \frac{\sigma_\mathrm{T}}{c} \cdot \frac{L}{4\pi r^2} \tag{6.12}$$

and therefore

$$L < L_\mathrm{Edd} = \frac{4\pi G M m_\mathrm{p} c}{\sigma_\mathrm{T}} \tag{6.13}$$

or, in astronomically meaningful units,

$$L < 1.3 \times 10^{38}\,\mathrm{erg\,s^{-1}} \cdot \frac{M}{M_\odot} \tag{6.14}$$

where L_Edd is called the Eddington luminosity.

But remember the assumptions entering the derivation: spherically symmetric accretion of fully ionized pure hydrogen gas.

Eddington luminosity, X

Characterize accretion process through the accretion efficiency, η:

$$L = \eta \cdot \dot{M} c^2 \tag{6.15}$$

where $\dot{M}$: mass accretion rate (e.g., g s^{-1} or $M_\odot$ yr^{-1}).

Therefore maximum accretion rate ("Eddington rate"):

$$\dot{m} = \frac{L_{\text{Edd}}}{\eta c^2} \sim 2 \times 10^{-8} \cdot \left(\frac{M}{1\, M_\odot} \right) M_\odot \,\text{yr}^{-1} \tag{6.16}$$

(for $\eta = 0.1$)

Emitted spectrum

Characterize photon by its radiation temperature, T_{rad}:

$$h\nu \sim k T_{\text{rad}} \quad \Longrightarrow \quad T_{\text{rad}} = h\nu / k \tag{6.23}$$

Optically thick medium: blackbody radiation

$$T_{\text{b}} = \left(\frac{L}{4\pi R^2 \sigma_{\text{SB}}} \right)^{1/4} \tag{6.24}$$

Optically thin medium: L directly converted into radiation without further interactions $\Longrightarrow$ mean particle energy

$$T_{\text{th}} = \frac{G M m_{\text{p}}}{3kR} \tag{6.25}$$

Plugging in numbers for a typical solar mass compact object (NS/BH):

$$T_{\text{rad}} \sim 1\,\text{keV} \quad \text{and} \quad T_{\text{bb}} \sim 50\,\text{MeV} \tag{6.26}$$

Accreting objects are broadband emitters in the X-rays and gamma-rays.

Emitted spectrum

Within the most simple of accretion disks, the potential energy gained by matter falling inwards is radiated away "on the spot".

Energy released by ring at radius r with width Δr:

$$L(r) = -\frac{\mathrm{d}E}{\mathrm{d}t} = \frac{3}{2} \frac{G\dot{M}M}{r^2} \Delta r \tag{6.27}$$

Factor $3/2$ takes change of Kepler speed into account.

If disk is optically thick, then both sides of disk radiate like a black body:

$$L(r) = 2 \cdot \sigma_{\text{SB}} T(r)^4 \cdot 2\pi r \Delta r \tag{6.28}$$

such that

$$T(r) = \left(\frac{3G\dot{M}M}{8\pi\sigma_{\text{SB}}} \right)^{1/4} \cdot r^{-3/4} \tag{6.29}$$

Emitted spectrum

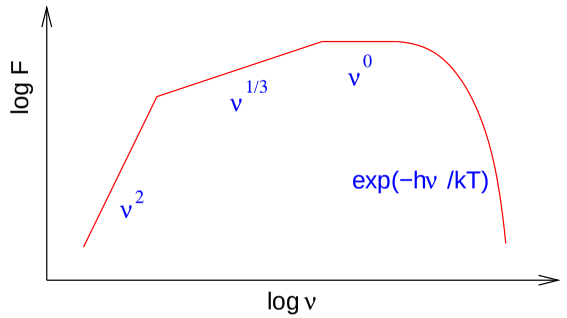

If disk is optically thick, then locally emitted spectrum is black body.

Total emitted spectrum obtained by integrating over disk

$$F_\nu = \int_{R_*}^{R_{\text{out}}} B(T(R))\, 2\pi R\, dR \tag{6.30}$$

Resulting spectrum looks essentially like a stretched black body.

Introduction

X-ray binaries are classified according to the nature of the compact object:

- Neutron Star X-ray Binaries (NS-XRBs)
- Black Hole X-ray Binaries (BH-XRBs or BHBs)
- (Cataclysmic Variables [accreting White Dwarfs]; CVs)

X-ray binaries are *also* classified according to the nature of the donor star:

- Low Mass X-ray Binaries (LMXBs)
- High Mass X-ray Binaries (HMXBs)

We will now look at these different types in more detail.

This is a rough overview only, for the details, see the separate Lecture on X-ray Binaries.

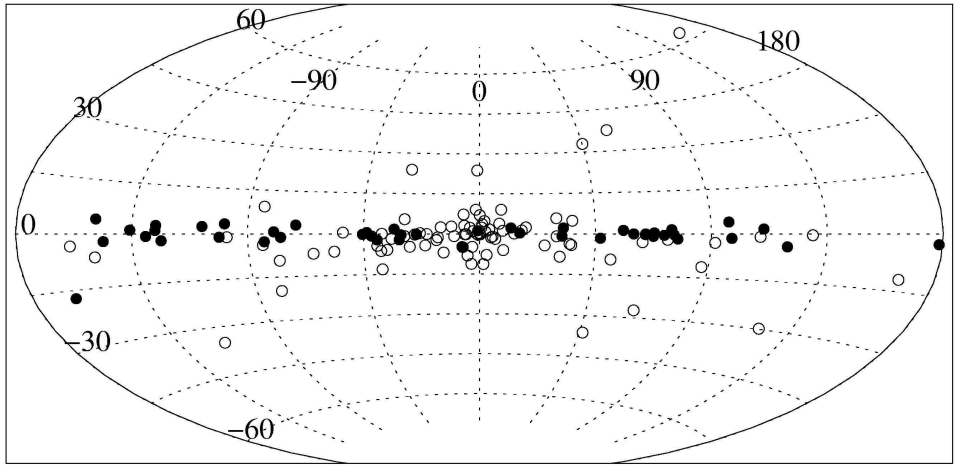

(Grimm, Gilfanov & Sunyaev, 2003)

Distribution of HMXB (filled circles) and LMXB (open circles) in the Galaxy

$\Longrightarrow$ HMXB: young systems $\longrightarrow$ disk population

$\Longrightarrow$ LMXB: also older systems seen at higher Galactic latitudes.

Neutron Star LMXBs, I

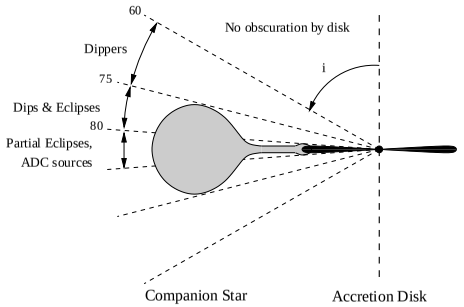

(after Charles & Seward, 1995, Fig. 8.3)

Low-Mass X-ray Binaries: Donor star has late spectral type (A and later), i.e. $M \lesssim 1.2\, M_\odot$.

$\Longrightarrow$ No stellar wind, systems are dominated by Roche Lobe overflow. Observed phenomenology mainly due to neutron star and the accretion disk, depending on viewing angle.

$\Longrightarrow$ Optical appearance: accretion disk and X-ray heated surface of donor star.

Objects in which the accretion process is most simple are the older neutron stars in low mass X-ray binaries (LMXBs).

These systems have low B-fields

$\Longrightarrow$ no pulsations observed

X-ray behavior depends strongly on the viewing angle.

Table 1 Bright low-mass X-ray binaries[a]

Source name(s)	l^{II}, b^{II} (°)	I_x[b] Mean (μJy)	Min. (μJy)	Max. (μJy)	P_{orb}[c] (hr)	Type[d]	Phenomenology[e]
Sco X-1 (1617−155)	359+24	12,400	9300	16,300	19.2	Z	QPO
GX 5−1 (1758−250)	5−1	1200	1070	1410	—	Z	QPO
GX 349+2 (1702−363)[f]	349+3	780	620	980	—	Z	QPO
GX 17+2 (1813−140)	16+1	680	600	780	19.8?[g]	Z	QPO, (bu)
GX 9+1 (1758−205)	9+1	650	550	720	—	A	—
GX 340+0 (1642−455)	340−0	490	400	620	—	Z	QPO
GX 3+1 (1744−265)	2+1	430	230	550	—	A	QPO, (Bu)
Cyg X-2 (2142+380)	87−11	430	290	730	235	Z	QPO, (bu), Mo
GX 13+1 (1811−171)	14+0	340	240	430	—	A	—
GX 9+9 (1728−169)	8+9	290	230	340	4.2	A	Mo
4U 1820−30 (NGC 6624)	3−8	260	94	360	0.2	A	QPO, (Bu), Mo
4U 1705−44	343−2	260	39	440	—	A	Bu
4U 1636−53	333−5	220	100	320	3.8	A	Bu
Ser X-1 (1837+049)	36+5	200	150	290	—	—	Bu
GCX-1 (1742−294)	0−0	170	130	270	—	—	Bu?
4U 1728−33	354−0	170	140	190	—	A	Bu
GX 339−4 (1659−487)	339−4	160	36	250	14.8?	—	QPO, BH?[h]
4U 1735−44	346−7	160	110	210	4.6	A	Bu

[a] All variable objects in 3A Catalogue (69, 153) with an average flux ≥100 μJy not identified with an early-type star (excluding Cyg X-3).
[b] Converted from *Ariel V* ASM counts into μJy (2–11 keV) according to 1 ASM c/s = 2.6 μJy (9).
[c] See (84).
[d] Z or A(toll) source; see text. After (36).
[e] QPO: all reported quasi-periodic oscillations are indicated here (see Section 3 for an evaluation of QPO reports in atoll sources); Bu: regular X-ray bursts; (Bu): has shown an episode of regular X-ray bursts; (bu): occasional X-ray bursts reported; BH?: black hole candidate, Mo: shows periodic X-ray modulation (9, 55, 64).
[f] "Sco X-2."
[g] Reference: (37).
[h] References: (77, 157).

(van der Klis, 1989, Tab. 1)

Classification

Hasinger & van der Klis (1989): “Two patterns of correlated X-ray timing and spectral behaviour in low-mass X-ray binaries”

Source classification through their behavior in the color-color-diagram or in the Hardness-Intensity-Diagram:

Here, we define an X-ray color (or “hardness ratio”):

$$\text{color} = \frac{\text{CR}_{\text{upper energy band}}}{\text{CR}_{\text{lower energy band}}} \qquad (6.31)$$

where CR_i is the measured count rate in a given energy band.

Typical bands used depend on the satellite, typical width is a few keV!

Z-sources

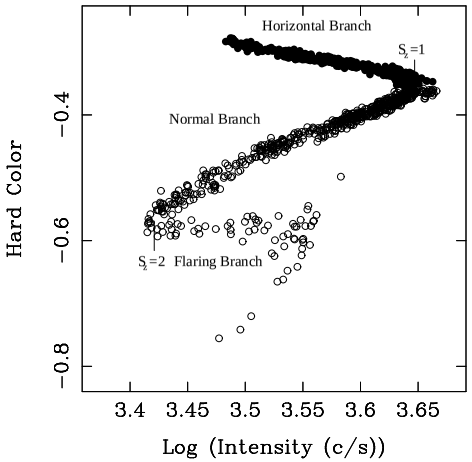

(GX 340+0; Jonker et al., 2000)

Z-sources: higher luminosity LMXBs (L_X close to L_{Edd}).

Color-intensity-diagram:

- horizontal branch: characterized by 20–50 Hz “Horizontal Branch Oscillations” (HBOs) and strong variability (including quasi-periodic oscillations, QPOs)
- normal branch: much weaker variability

  pre 1988 people thought this behavior to be the normal one for neutron star LMXB.
- flaring branch: spectrum mostly thermal

  Named after flares in Sco X-1

Intensity described with S_Z-parameter along the Z.

Atoll sources

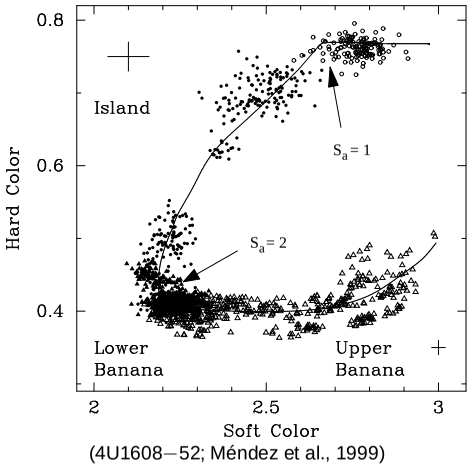

(4U1608−52; Méndez et al., 1999)

Atoll sources: generally lower luminosity than Z-sources; color-color-diagram looks like a pacific island

Intensity increases with parameter S_a:

- banana state: higher luminosity state, variability dominated by low frequency noise
- island state: lower luminosity state, variability dominated by high frequency noise

S_a is defined “by eye”, see diagram

Typical luminosities 0.01–0.2 L_{Edd}, although four sources might be brighter than that (van der Klis, 2000)

Spectral shape, I

(White, Stella & Parmar, 1988): The spectral shape is well described by a power law with exponential cutoff,

$$N_{\text{ph}}(E) \propto E^{-\Gamma} \exp\left(-\frac{E}{E_{\text{fold}}}\right) \qquad (6.32)$$

where

- N_{ph}: photon flux (ph cm^{-2} s^{-1} keV^{-1}),
- $\Gamma \sim$ 0–2: photon index,
- $E_{\text{fold}} \sim$ 1–20 keV: folding energy (also often called cutoff energy)

Such a spectral shape probably due to Comptonization

High luminosity sources (=Z-sources) show additional black body component with $kT_{\text{BB}} \sim$ 1–2 keV, contributing 10–70% of the total flux (higher L_X implies more BB-flux).

Often, an additional Fe Kα line at 6.4 keV is required.

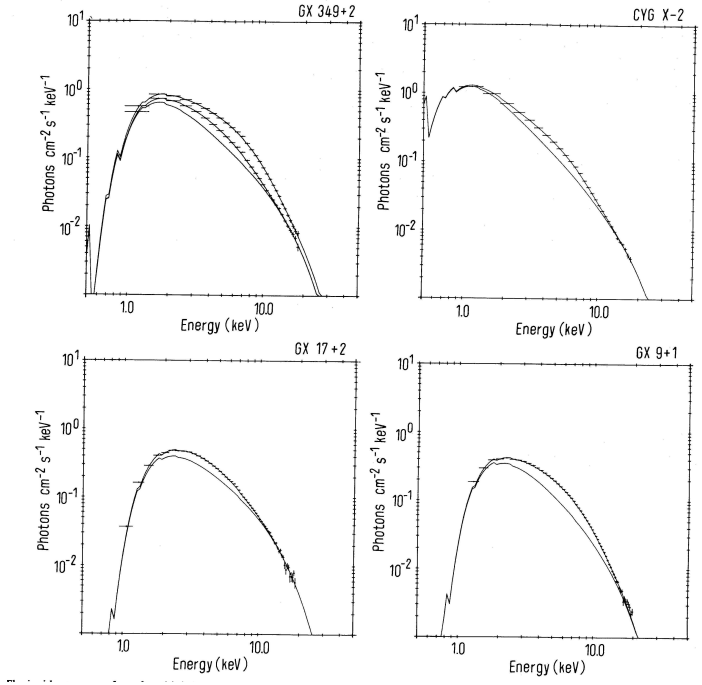

Example spectra of LMXB (White, Stella & Parmar, 1988, lower line is Comptonization only)

Spectral shape, III

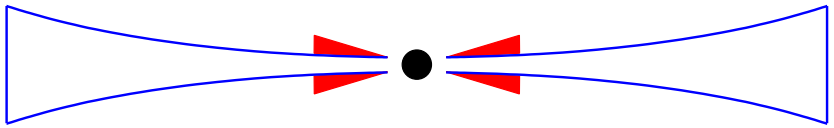

(after Church, 2004)

The interpretation of spectral shape is heavily debated.

Western model (White, Stella & Parmar, 1988) and Birmingham model (Church & Balucinska-Church, 1995):

- black body is from neutron star,
- Comptonization happens in inner edge of the accretion disk (e.g., in hot accretion disk wind).

Spectral shape, IV

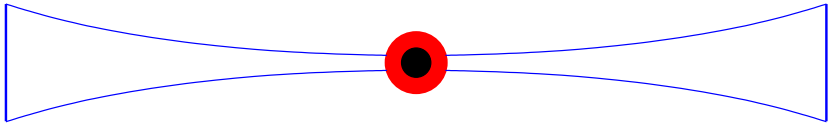

(after Church, 2004)

The interpretation of the spectral shape is heavily debated.

Eastern model (Mitsuda et al., 1989):

- Soft spectrum: thermal radiation from accretion disk
  (assuming $T(r) \propto r^{-3/4}$)
- Hard spectrum is Comptonization in neutron star atmosphere (which provides seed photons as thermal radiation).

QPOs

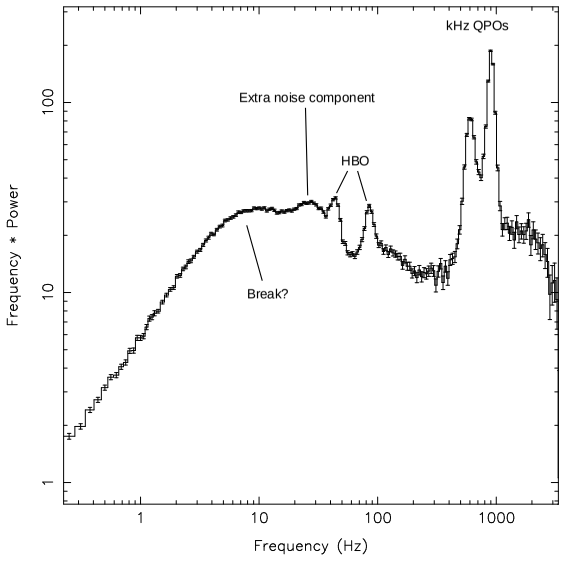

Arguably, the most fascinating phenomen seen in NS-LMXBs are Quasi Periodic Oscillations in the kHz range:
"The kHz QPO are the most important scientific result to date of RXTE" (NASA).

Power spectrum (=squared Fourier transform) of the lightcurve of Sco X-1; van der Klis et al., 1996, IAUC 6319, Wijnands & van der Klis (1999)

QPOs

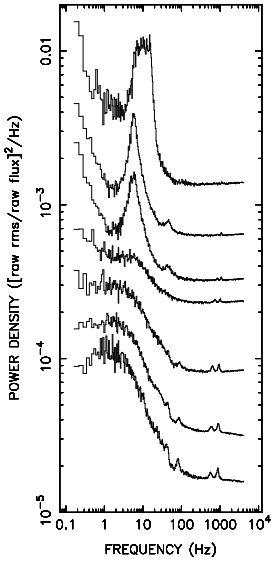

- always have 3 characteristic frequencies:
  - "Low Frequency QPOs" ($\nu_{\rm LF}$): 0.1–100 Hz, many types
  - "kHz Twin Peaks" (ν_1, ν_2): 200–1400 Hz
- "real" kHz QPOs only for neutron star binaries, mostly persistent LMXBs,
  $\gtrsim$ 20 kHz QPO sources are known, mostly showing twin peaks

The kHz QPO strength is flux dependent.

(Wijnands & van der Klis, 1999)

QPOs

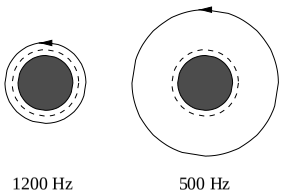

1200 Hz 500 Hz

kHZ QPOs occur on timescales close to the innermost stable circular orbit:
The Keplerian orbit frequency: is

$$\nu_{\rm orb} = \left(\frac{GM}{4\pi^2 R_{\rm orb}^3}\right)^{1/2} \approx 1200\,{\rm Hz}\left(\frac{R_{\rm orb}}{15\,{\rm km}}\right)^{-3/2} m_{1.4}^{1/2} \qquad (6.33)$$

The edge of the accretion disk is at the innermost stable circular orbit (ISCO), Schwarzschild geometry:

$$R_{\rm ISCO} = \frac{6GM}{c^2} \sim 12.5 M_{1.4}\,{\rm km} \qquad (6.34)$$

and therefore the maximum stable frequency in an accretion disk is

$$\nu_{\rm ISCO} \sim \frac{1580\,{\rm Hz}}{M_{1.4}} \qquad (6.35)$$

Corrections due to the spin of the central object can amount to several 10%

QPOs

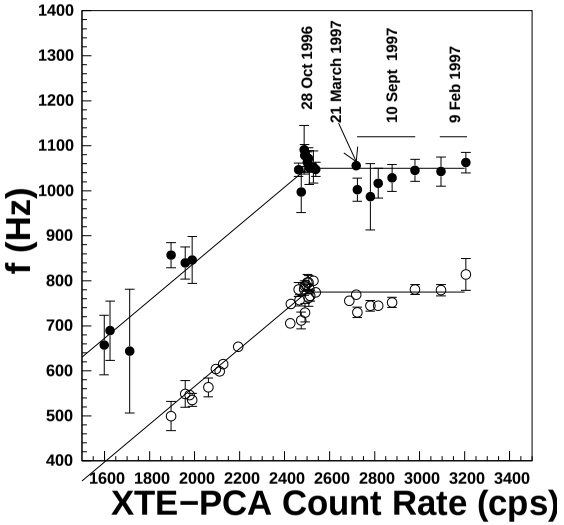

The frequencies of kHz QPOs usually increase with X-ray flux ("parallel-lines phenomenon"), and can saturate at a maximum frequency.

$\Longrightarrow$ Models need to explain $\nu_{\rm LF}$, ν_1, and ν_2.

(4U 1820−30; Zhang et al., 1998)

QPOs

Beat Frequency Model:

"beat": resonance between some preferred Keplerian orbit & spin frequency

Magnetospheric BFM:

- preferred radius = Alfvén radius
- orbiting clump ($\nu_{\rm Alfvén}$) modulated by B-field ($\nu_{\rm spin}$)

$\Longrightarrow$ can explain LF QPOs, 5–50 Hz

Sonic Point BFM:

- preferred radius = where radial inflow velocity becomes supersonic, near ISCO
- orbiting clump ($\nu_{\rm sonic} > \nu_{\rm spin}$) causes bright footpoint near surface, footpoint: upper kHz QPO, $\nu_2 = \nu_{\rm sonic}$
- clumps are irradiated with $\nu_{\rm spin}$
  $\Longrightarrow$ footpoint emission is modulated with beat between $\nu_{\rm sonic}$ and $\nu_{\rm spin}$, footpoint modulation: lower kHz QPO, $\nu_1 = \nu_{\rm beat}$

QPOs

Relativistic Precession Model:

General Relativity: free-particle orbits show characteristic frequencies

Idea of the model:

- disk is disrupted near ISCO, forming blobs
- blob orbits are inclined and eccentric

Characteristic frequencies:

- orbit frequency: upper kHz QPO, ν_2
- periastron precession: lower kHz QPO, ν_1
- relativistic frame dragging $\rightarrow$ "wobble of the orbital plane":
  nodal precession (Lense-Thirring)
  $\nu_{\rm LF} = 2 \times \nu_{\rm nod}$

$\nu_{\rm nod} = 8\pi^2 I\, \nu_2^2 \nu_{\rm spin} / c^2 M$, where I: moment of inertia

see, e.g., Stella & Vietri (1998)

QPOs

Promises:

- constrain M and R (via kHz QPOs)
  $\Longrightarrow$ constrain Equation of State for neutron stars
- constrain spin
  ("holy grail", LMXB/ms radio pulsar evolution?!)
- constrain B-field (via LF QPOs)
- observe GR effects

Difficulties:

- observations (varying $\Delta\nu_{\rm kHz}$, ν-correlations)
  triggered evolution of many different models (> 12)
- no individual model does address all issues
  (i.e, generation of flux modulation, ...)
- models predict different $\nu_{\rm spin}$ and M, e.g.,
  BFM: $\nu_{\rm spin} = 250$–$350\,$Hz
  RPM: $\nu_{\rm spin} = 300$–$900\,$Hz
- what about "surface models"? $\Longleftrightarrow$ big question: do BHCs show the same behavior as neutron star XRBs?